

Atomic and molecular signatures for charged-particle ionization

Ola Al-Hagan¹, Christian Kaiser², Don Madison^{1*} and Andrew James Murray^{2*}

The way in which atoms and molecules are ionized by the impact of charged particles has important consequences for the behaviour of many physical systems, from gas lasers to astrophysical plasmas. Much of our understanding of this process has come from ionization measurements of the energy and angular distribution of electrons ejected in the same plane as the trajectory of the incident ionizing beam. Such studies suggest that the mechanisms governing the ionization of atoms and molecules are essentially the same. But by measuring the electrons ejected from a gas in a plane perpendicular to the incident beam, we show this is not always the case. Experiments and quantum mechanical calculations enable us to construct a remarkably accurate classical picture of the physics of charged-particle ionization. This model predicts that the differences in ionization behaviour arise in molecules that do not have nuclei at their centres of mass.

The most sophisticated experiments being carried out at present measure the ionization probability as a function of the outgoing projectile and ejected electron momenta^{1–4}. These measurements, called differential cross-sections (DSCs), provide very sensitive tests for theory. Theoretical models for low to intermediate energies (where the ionization probability is highest) must consider many factors, including distortions in the wavefunctions describing the projectile and target, target polarization due to the Coulomb interaction between the incident projectile, nucleus and bound electrons, exchange effects, multiple scattering and post-collision interactions between particles emerging from the reaction. The most sophisticated theories include all of these processes, and compare well to experimental data for atomic targets such as hydrogen^{5–7}, helium⁸, the noble gases^{9–13} and alkali and alkali-earth metals^{14,15}.

A common experimental arrangement is to fix the scattered projectile energy and angular location, and then measure the probability that the ejected electron emerges at different angles in a plane determined by the initial and final momentum of the projectile (called the coplanar scattering plane, $\psi = 0^\circ$ in Fig. 1). These measurements show that there is a large probability for ejecting the target electron in the direction of the projectile momentum change (this is for ionization of *s* states; for *p* states, this peak may split into two lobes centred on the direction of momentum change), and a smaller probability that the electron is ejected opposite to this direction¹⁶. In the first feature, the ejected electron moves in a direction that conserves momentum for the projectile-ejected electron system, and so this is attributed to a classical binary collision between these two particles, which is then called the binary peak. The second feature is attributed to a binary collision sending the atomic electron in the direction of momentum transfer, followed by an elastic 180° backscattering from the nucleus. This second feature containing a double collision process is called the recoil peak because the nucleus must recoil to conserve momentum. Binary and recoil peaks are the dominant features in all ionizing collisions, and are found for all projectiles and for all atomic and molecular targets.

Experimental arrangement and results

Here, we report an investigation of ionization in a plane perpendicular to the incident beam direction ($\psi = 90^\circ$ in Fig. 1) using electrons as projectiles and atomic helium and molecular hydrogen as targets. Figure 2 shows the experimental data for electron impact ionization of He and H₂ in the perpendicular plane, where the outgoing electron energies are $E_a = E_b = 10$ eV (the incident electron energy is 44.6 eV for He and 35.6 eV for H₂). As neutral He and H₂ have an equivalent number of protons and electrons, these results markedly contrast the difference in distribution of the constituents that make up these atomic and molecular targets. For He, three peaks are observed as a function of the angle $\varphi = \theta_a + \theta_b$ (see Fig. 1), with a large central peak at $\varphi = 180^\circ$ (two electrons leaving back-to-back) and clearly resolved smaller peaks at $\varphi \sim 90^\circ, 270^\circ$ (the three-lobe atomic helium structure has previously been observed for different kinematics¹⁷). Similar to He, we find peaks in the vicinity of $\varphi \sim 90^\circ, 270^\circ$ for ionization of H₂. However, instead of a maximum for back-to-back scattering as in He, we find a minimum at $\varphi = 180^\circ$. This difference must be due to either the nuclear configuration of H₂ compared with He, or to the different bound-state electron momentum distributions. The data clearly show the sensitivity of measurements in this geometry. It should be noted that experimental results in a coplanar geometry in this energy regime are very similar for both targets, which means the marked differences between atoms and molecules seen here are not observable in the usual coplanar geometry adopted by most researchers.

Possible types of collision

It is instructive to consider classically how the projectile–target interaction can produce ionization into the perpendicular plane. First, consider only binary collisions between the projectile and the target electrons, ignoring the nuclei. If we look at the 180° case, where there is a large difference between atoms and molecules, the two final-state electrons have equal energies and are moving in opposite directions such that the net final-state momentum is zero. This means that, in the initial state, the bound-state electron

¹Department of Physics, Missouri University of Science and Technology, Rolla, Missouri 65409, USA, ²School of Physics and Astronomy, University of Manchester, Manchester M13 9PL, UK. *e-mail: madison@mst.edu; Andrew.Murray@manchester.ac.uk

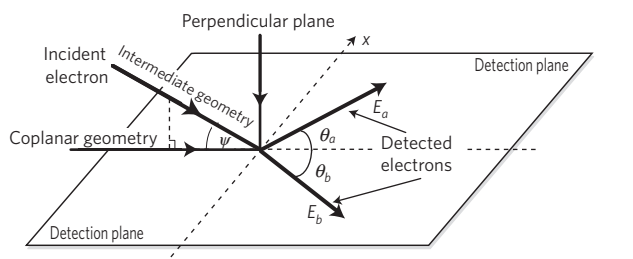


Figure 1 | The experimental geometry. A plane is defined by the detected electrons. The incident-electron gun can move from a coplanar geometry ($\psi = 0^\circ$) to the perpendicular plane ($\psi = 90^\circ$), where the angle $\varphi = \theta_a + \theta_b$ is defined. A common point between all planes occurs when $\theta_a = \theta_b = \pi/2$.

momentum \mathbf{k}_{bd} would need to be opposite to the initial projectile momentum \mathbf{k}_{in} , as shown in Fig. 3a. For back-to-back final-state electron measurements, this is the only process leading to ionization into the perpendicular plane that does not involve the nucleus.

If we include the nucleus in our model, it is possible for the projectile electron to enter the perpendicular plane by first undergoing a small-impact-parameter elastic collision with the nucleus, followed by a classical binary collision with the atomic electron, so that both electrons emerge in the perpendicular plane. In this case, a binary collision will tend to cause the two electrons to emerge at a relative angle of $\varphi \sim 90^\circ$ owing to their equal mass (Fig. 3b). For spherically symmetric targets, scattering into this plane must be symmetric around \mathbf{k}_{in} , resulting in peaks at $\varphi \sim 90^\circ, 270^\circ$ as seen for both He and H₂.

For this process to produce back-to-back ($\varphi \sim 180^\circ$) electrons, we must have an extra scattering from the nucleus. As small impact parameters are required to bring the projectile into the perpendicular plane (of the order of $0.5a_0$, where $a_0 \sim 0.53$ nm is the Bohr radius), one of the electrons (\mathbf{k}_a) may also re-scatter from the nucleus so as to emerge in a direction opposite the other electron (\mathbf{k}_b) after the binary collision occurs (Fig. 3c). As this happens on either side of the nucleus with equal probability, a peak centred at $\varphi = 180^\circ$ results. Other second- and higher-order processes involving nuclear scattering may also occur.

Quantum mechanical calculation

Although these simple classical pictures are very appealing, atomic and molecular ionization is fundamentally a quantum mechanical process. It is however possible to use quantum mechanics to test these classical ideas. We can calculate the probability of these processes occurring quantum mechanically by evaluating a quantity called the T-matrix, which, in a three-body approximation, is given by:

$$T = \underbrace{\langle \chi_{\text{scat}} \chi_{\text{ej}} C_{\text{scat-ej}} \rangle}_{\text{Final state}} V \underbrace{|\varphi_{\text{bound}} \chi_{\text{in}} \rangle}_{\text{Initial state}}.$$

The T-matrix is an integral involving the initial and final states of the system and the interaction between the projectile and target (V). The initial state consists of the incoming projectile wavefunction (χ_{in}) and the bound-state wavefunction for the atomic or molecular electron (φ_{bound}) (we use numerical Hartree–Fock wavefunctions for either an atom or molecule). The final state consists of the scattered projectile wavefunction (χ_{scat}), the ejected electron wavefunction (χ_{ej}) and the Coulomb interaction between the scattered projectile and ejected electron ($C_{\text{scat-ej}}$) (we use a form first proposed by Ward and Macek¹⁸). For the calculations presented here, the wavefunctions for the free particles (χ) are called distorted waves. Distorted waves are solutions of the Schrödinger equation for a spherically symmetric potential representing either the atom or molecule. The important physics contained in the distorted

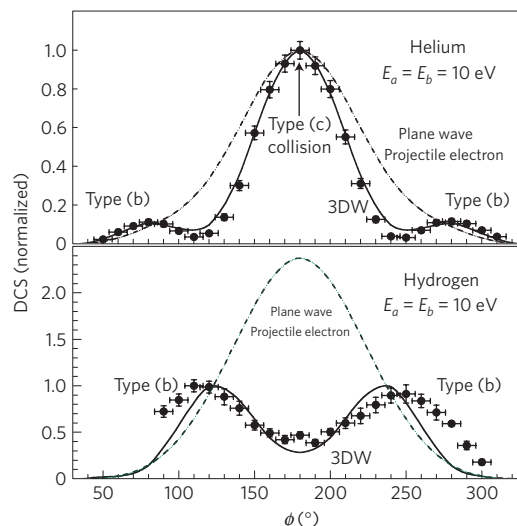


Figure 2 | Experimental and theoretical DCS data in the perpendicular plane for He and H₂ targets, normalized to unity at the experimental maximum. The outgoing energies were $E_a = E_b = 10$ eV in both cases. The results show the significant differences between ionizing atomic and molecular targets, and contrast the effects of using plane and distorted waves to describe the projectile electron. Error bars in the DCS indicate the statistical variation measured over a series of sweeps of the analysers around the detection plane. Horizontal error bars show the estimated angular response of the spectrometer due to the analyser entrance apertures and the incident electron beam pencil angle. The type of collision process noted in this figure is described in Fig. 3.

wave is elastic scattering from the target. Consequently, (χ_{in}) is a wavefunction representing elastic scattering from a neutral target and ($\chi_{\text{scat}}, \chi_{\text{ej}}$) are wavefunctions representing elastic scattering from an ion.

As current experiments using molecules do not determine the orientation of the molecule at the time of ionization, an average over all orientations must be made. We approximate this by calculating an elastic scattering potential for molecules obtained by averaging the bound-state electron charge density over all orientations, and by averaging the two nuclei over all orientations. For H₂, the two protons are separated by $1.4a_0$, and so we approximate averaging over all molecular orientations by assuming the nuclear charge of $+2$ is uniformly distributed on a spherical shell with a radius of $0.7a_0$ (see Fig. 4). The approximate form of the T-matrix we use is called the three-body distorted wave (3DW) model^{19,20}. The 3DW results for ionization of He and H₂ are compared to experiment in Fig. 2. As the data are not absolute, experiment and theory are each scaled to unity at their highest value. The agreement between experiment and theory is clearly very good.

Using quantum mechanics to identify collision types

The key objective of this work is to understand the underlying physical effects producing both similarities and differences between atomic and molecular targets. There are two components to the theoretical calculation—the bound-state wavefunctions (φ_{bound}) and wavefunctions describing the electrons in the continuum (χ). If the mechanism in Fig. 3a is the main contributor to the maximum at $\varphi \sim 180^\circ$ for He and also produces the minimum in H₂, this must be due to the bound-state wavefunctions, as they contain the initial-state momentum distributions \mathbf{k}_{bd} of the bound electrons. To determine the importance of the momentum distribution in H₂, we repeated the H₂ calculation by replacing the molecular H₂ wavefunction (φ_{H_2}) with a He wavefunction (φ_{He}) (leaving everything else unchanged for the molecule). The result of these

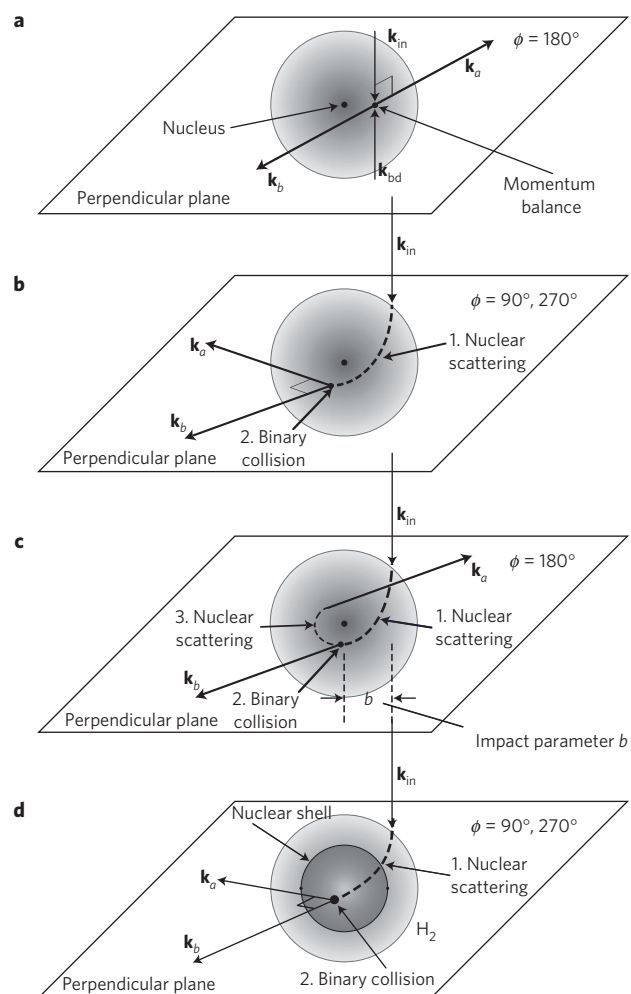


Figure 3 | Different mechanisms that may lead to ionization in the perpendicular plane. **a**, The only mechanism that can occur without nuclear scattering. **b**, The effect of nuclear scattering followed by a binary collision, leading to peaks at $\phi \sim 90^\circ, 270^\circ$. **c**, The triple scattering process that leads to a central peak at $\phi \sim 180^\circ$ for targets that have a nucleus at the centre of mass. **d**, The effect of distributing the nuclear charge on a thin shell, in which case the mechanism in **c**, cannot occur.

calculations again produced a minimum at $\phi = 180^\circ$. This clearly indicates that the mechanism in Fig. 3a is not the primary source of the differences between He and H₂ at this angle.

The mechanisms shown in Fig. 3b,c both require elastic scattering from the target. As noted above, the free-particle distorted waves we use are elastic scattering wavefunctions from the target. A wavefunction that does not contain elastic scattering from the target is a free-particle plane wave. Consequently, we can determine the effect of elastic scattering of the projectile from the target by replacing (χ_{in}, χ_{scat}) by plane waves. The results of these calculations are also shown in Fig. 2, where it is seen that elastic scattering of the projectile from the target produces the peaks near 90° and 270° for both H₂ and He. The 90° and 270° peaks for He have been observed previously for different kinematics¹⁷, and Zhang *et al.*²¹ carried out a detailed study for ionization of He into the perpendicular plane. They proposed this method for identifying the physical mechanisms of the collision. We hence conclude that the mechanism in Fig. 3b is responsible for these outlying structures in both atomic He and molecular H₂ targets and speculate that these features are generic for atomic and molecular targets.

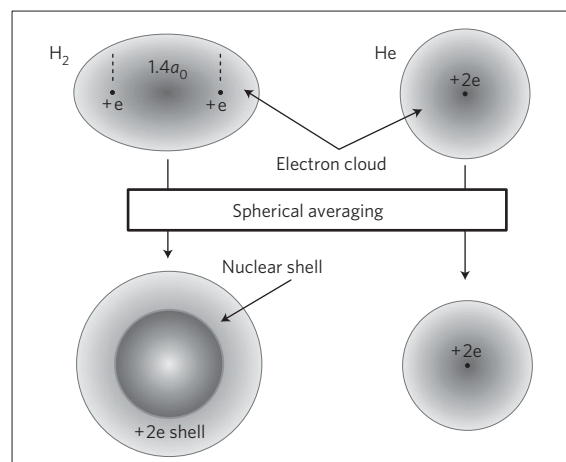


Figure 4 | Averaging of the electronic and nuclear structure of the targets as experimental constraints mean that the orientation of the molecule cannot be determined. For H₂, the nuclear charge is distributed on a thin shell of diameter 1.4 Bohr radii, whereas for He the charge is concentrated at the centre of the target.

Nuclear distribution causes the difference

The most striking observation is the difference seen at $\phi = 180^\circ$. The source of this feature must lie in the difference between elastic scattering wavefunctions for atoms and molecules, as distorted waves give a peak for He and a minimum for H₂. Given that these wavefunctions contain elastic scattering from the bound-state electrons as well as elastic scattering from the nuclei, we investigated the electronic and nuclear contributions individually and found the important difference lies in the treatment of the nuclei (described as a point charge for He and a thin spherical shell of charge for H₂, as discussed above).

To investigate the importance of the size of the nuclear shell for H₂, calculations were repeated with the shell size reducing from $R = 0.7a_0$ to a point charge (while keeping the electronic component unchanged). The marked changes in the predicted results are seen in Fig. 5. As the shell diameter decreases, the minimum at $\phi = 180^\circ$ becomes deepest at $0.5a_0$, after which a maximum appears, which is largest for a point charge ($R = 0.0a_0$). The H₂ results are then very similar to that for He when the nuclear charge is concentrated at a single point, indicating that the distance between the nuclei has a critical role in determining the ionization probability for back-to-back scattering. We also carried out a similar calculation for He. In this case, we replaced the point charge with a charge of +2 on a sphere of increasing size while leaving everything else the same. Again, we found that the maximum at 180° quickly developed into a minimum. It is therefore clear that the 180° minimum stems from the separated nuclei in the molecule.

The effect of shell size on the peak at $\phi = 180^\circ$ indicates this feature is dominated by the processes shown in Fig. 3c,d. If classical Rutherford scattering theory is used to equate the impact parameter b with scattering angle, it is found that $b = 0.4a_0 - 0.6a_0$ is required to elastically scatter into the perpendicular plane for the present kinematics. For He, the projectile (or ejected) electron following the binary collision is then close to the nucleus so it has a strong attraction to the point nucleus, and preferentially backscatters elastically as in Fig. 3c. For H₂, the electrons are mostly inside the spherical shell at the time of the binary collision (Fig. 3d), so experience no attractive force that would produce a peak at $\phi = 180^\circ$. For binary collisions within the shell, the Coulomb force from the nuclei is zero, so the electrons will then leave at a mutual angle $\phi \sim 90^\circ$.

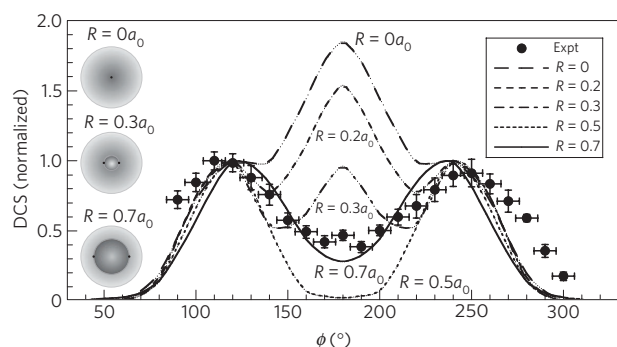


Figure 5 | Change in the calculated ionization DCS for H_2 in the perpendicular plane as a function of the size of the spherically averaged nuclear shell, normalized to unity at the experimental maximum. Error bars are as described in Fig. 2.

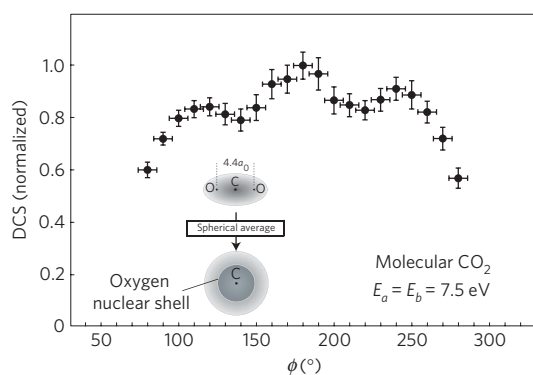


Figure 6 | DCS for ionization of CO_2 in the perpendicular plane normalized to unity at the experimental maximum. A maximum is seen at $\phi = 180^\circ$, as found for He, in contrast to the results from H_2 . This is attributed to the carbon nucleus being at the centre of mass of the molecule, so that spherical averaging produces an oxygen nuclear shell with an extra nuclear target at the centre of the molecule. The scattering process shown in Fig. 3c can then take place from this carbon nucleus. Error bars are as described in Fig. 2.

The question arises of why there is a peak at 180° for He resulting from backscattering from the nucleus when all scattering angles should be equally likely. This is of course true only if all impact parameters are equally likely. However, for the present kinematics following the binary collision, the electrons have energy ~ 10 eV and an impact parameter between $0.4a_0$ and $0.6a_0$. Again using Rutherford scattering from a point charge, the resulting scattering angles range from 150° to 160° for these values. As there is an equal probability of left and right scattering, the resulting signal will be distributed between $\pm 150^\circ$ centred around $\phi = 180^\circ$, as is observed.

Although these classical descriptions of ionization aid in explaining the differences between He and H_2 and highlight the importance of the nuclear configuration, the fully quantum mechanical calculation is of course needed to accurately describe the data. It is intriguing to note that the nuclear configuration has such a crucial role in the observed structures in the perpendicular plane, whereas it has almost no role for the binary and recoil peaks seen in a coplanar geometry (where most previous measurements have been made).

Generalizing the model to larger molecules

The minimum in the cross-section for 180° scattering in the perpendicular plane found for H_2 has been attributed here to the fact that the binary collisions are taking place in a force-free region

inside a spherical shell of charge. This spherical shell of charge resulted from averaging over all molecular orientations. The present results suggest that a minimum would be found for any diatomic molecule or perhaps for any molecule that does not have a nucleus located at the centre of mass. Conversely, molecules that have a nucleus at the centre of mass might then be expected to act in a similar way to an atom. To test this conjecture, experimental results for ionization of the $1\pi_g$ state of CO_2 in the perpendicular plane are presented in Fig. 6, where it is seen that we find a broad maximum at 180° instead of a minimum. Consequently, these results strongly suggest that molecules that have no nuclei at the centre of mass will have a minimum for back-to-back scattering and molecules that have a nucleus at the centre of mass will have a maximum, as is found for atoms.

Received 23 April 2008; accepted 11 October 2008;
published online 16 November 2008

References

- Dürr, M., Dimopoulou, C., Najjari, B., Dorn, A. & Ullrich, J. Three-dimensional images for electron-impact single ionization of He: Complete and comprehensive (e,2e) benchmark data. *Phys. Rev. Lett.* **96**, 243202 (2006).
- Casagrande, E. M. S. *et al.* New coplanar (e,2e) experiments for the ionisation of He and Ar atoms. *J. Electron Spectrosc. Relat. Phenom.* **161**, 27–30 (2007).
- Lower, J. R., Bellm, S. & Weigold, E. An improved double-toroidal spectrometer for gas phase (e,2e) studies. *Rev. Sci. Instrum.* **78**, 111301 (2007).
- Deharak, B. A. & Martin, N. L. S. An out-of-plane (e, 2e) spectrometer using a movable electron gun. *Meas. Sci. Tech.* **19**, 015604 (2008).
- Bray, I. & Stelbovics, A. Explicit demonstration of the convergence of the close-coupling method for a Coulomb three-body problem. *Phys. Rev. Lett.* **69**, 53–56 (1992).
- Rescigno, T. N., Baertschy, M., Isaacs, W. A. & McCurdy, C. W. Collisional breakup in a quantum system of three charged particles. *Science* **286**, 2474–2479 (1999).
- Colgan, J., Pindzola, M. S., Robicheaux, F. J., Griffin, D. C. & Baertschy, M. Time-dependent close-coupling calculations of the triple-differential cross section for electron-impact ionization of hydrogen. *Phys. Rev. A* **65**, 042721 (2002).
- Bray, I., Fursa, D. V. & McCarthy, I. E. Convergent close-coupling method for electron scattering on helium. *J. Phys. B* **27**, L421–L425 (1994).
- Murray, A. J. & Read, F. H. Evolution from the coplanar to the perpendicular plane geometry of helium (e,2e) differential cross sections symmetric in scattering angle and energy. *Phys. Rev. A* **47**, 3724–3732 (1993).
- Murray, A. J. & Read, F. H. Low energy (e, 2e) differential cross section measurements on neon from the coplanar to the perpendicular plane geometry. *J. Phys. B* **33**, L297–L302 (2000).
- Rasch, J., Whelan, C. T., Allan, R. J., Lucey, S. P. & Walters, H. R. J. Strong interference effects in the triple differential cross section of neutral-atom targets. *Phys. Rev. A* **56**, 1379–1383 (1997).
- Stelbovics, A. T., Bray, I., Fursa, D. V. & Bartschat, K. Electron-impact ionization of helium for equal-energy-sharing kinematics. *Phys. Rev. A* **71**, 052716 (2005).
- Milne-Brownlie, D. S., Foster, M., Gao, J., Lohmann, B. & Madison, D. H. Young-type interference in (e, 2e) ionization of H_2 . *Phys. Rev. Lett.* **96**, 233201 (2006).
- Murray, A. J. (e, 2e) ionization studies of alkaline-earth-metal and alkali-earth-metal targets: Na, Mg, K, and Ca, from near threshold to beyond intermediate energies. *Phys. Rev. A* **72**, 062711 (2005).
- Srivastava, M. K., Kumar, R. C. & Srivastava, R. Coplanar doubly symmetric (e, 2e) process on sodium and potassium. *Phys. Rev. A* **74**, 064701 (2006).
- Schulz, M. *et al.* Three-dimensional imaging of atomic four-body processes. *Nature* **422**, 48–50 (2003).
- Murray, A. J., Woolf, M. B. J. & Read, F. H. Results from symmetric and non-symmetric energy sharing (e, 2e) experiments in the perpendicular plane. *J. Phys. B* **25**, 3021–3036 (1992).
- Ward, S. J. & Macek, J. H. Wave functions for continuum states of charged fragments. *Phys. Rev. A* **49**, 1049–1056 (1994).
- Gao, J., Peacher, J. L. & Madison, D. H. An elementary method for calculating orientation-averaged fully differential electron-impact ionization cross sections for molecules. *J. Chem. Phys.* **123**, 204302 (2005).
- Gao, J., Madison, D. H. & Peacher, J. L. Distorted wave born and three-body distorted wave born approximation calculations for the fully differential cross section for electron impact ionization of nitrogen molecules. *J. Chem. Phys.* **123**, 204314 (2005).

21. Zhang, X., Whelan, C. T. & Walters, H. R. J. Energy sharing ($e,2e$) collisions-ionisation of helium in the perpendicular plane. *J. Phys. B* **23**, L173–L178 (1990).

Acknowledgements

We thank the EPSRC (UK) for supporting these experiments, and the NSF for support of the theoretical work under grant No. PHY-0757749.

Author contributions

O.A.-H. and D.M. carried out the theoretical calculations for this work, whereas C.K. and A.M. carried out the experimental investigations that are presented.

Additional information

Reprints and permissions information is available online at <http://npg.nature.com/reprintsandpermissions>. Correspondence and requests for materials should be addressed to D.M. or A.J.M.